

High-sensitivity ultrashort mid-infrared pulse characterization by modified interferometric field autocorrelation

Ming-Sung Chao,¹ Hsiang-Nan Cheng,¹ Bo-Jyun Fong,² Zhi-Ming Hsieh,² Wei-Wei Hsiang,² and Shang-Da Yang^{1,*}

¹*Institute of Photonics Technologies, National Tsing Hua University, Hsinchu 30013, Taiwan*

²*Department of Physics, Fu Jen Catholic University, Taipei 24205, Taiwan*

*Corresponding author: shangda@ee.nthu.edu.tw

Received October 27, 2014; accepted January 6, 2015;
posted January 16, 2015 (Doc. ID 225299); published March 4, 2015

We report on spectral phase retrieval of 43 MHz, \sim 100 fs, 3.3 μ m pulses at energies down to 8.9 pJ by a modified interferometric field autocorrelation method. The simple setup consists of a Michelson interferometer, a 266 μ m thick AgGaSe₂ crystal, and a homemade spectrometer with an InGaAs point detector, which is readily applicable to measuring a 20 fs (1.8 cycles) pulse at 3.3 μ m. The feasibility is verified by comparing with the results obtained by simulation and frequency-resolved optical gating for the spectral phase modulation because of a 4 mm thick germanium plate. © 2015 Optical Society of America

OCIS codes: (320.7100) Ultrafast measurements; (320.7110) Ultrafast nonlinear optics.
<http://dx.doi.org/10.1364/OL.40.000902>

Ultrafast technologies in the mid-infrared (MIR) are receiving increasing attention because of the applications in high harmonic generation (HHG) [1], investigation of topological insulators [2], and two-dimensional infrared spectroscopy [3]. It is desirable to retrieve the temporal shape of the MIR ultrashort pulse, which typically has a profound impact on the experimental results (e.g., chirped pulses are inappropriate to produce isolated attosecond burst via HHG).

An excellent review about MIR pulse characterization techniques can be found in [4]. Autocorrelation and cross-correlation measurements were used in estimating the durations (50–150 fs) of MIR pulses centered at 3–20 μ m wavelengths [5], while the exact temporal shapes were unavailable. Electro-optic sampling successfully characterized the electric field of a 28 fs pulse at 8.9 μ m [6]. Nevertheless, it requires a synchronized reference pulse shorter than the carrier cycle of the test field (a 10 fs reference pulse was used in [6]).

In the presence of a visible or near-infrared (NIR) reference pulse whose duration is not much longer than the test MIR pulse, nonlinear signal acquisition can be greatly facilitated by up-converting the MIR spectrum to the CCD-sensitive range via sum-frequency generation (SFG). In this way, cross-correlation frequency-resolved optical gating (X-FROG) [7–9] and variants of spectral interferometry for direct e-field reconstruction (SPIDER) [4,10] characterized MIR pulses centered at 3.0–7.6 μ m and of durations ranging from 13 to 300 fs. In addition to the increased complexity, these reference-assisted techniques are subject to two common problems: (1) They are not readily applicable to pulses directly produced by mode-locked oscillators [11,12] for the lack of an inherent reference source; (2) The large group velocity mismatch (GVM) among the MIR, reference, and up-converted pulses could seriously distort the SFG spectrum [13] (thus restricting the measurable pulse width), and even the thinnest crystal and angle dithering are employed [8,9].

In terms of self-referenced methods, a second-harmonic-generation (SHG) FROG and a time-domain

homodyne optical technique (HOT) SPIDER have been applied to measuring \sim 100 fs MIR pulses at 3.2 μ m and 9 μ m, respectively [14,15]. Nevertheless, a nonlinear crystal with a smaller effective nonlinear coefficient (AgGaS₂, $d_{eff} = 9.11$ pm/V) and a costly spectrometer with a built-in InGaAs detector array were employed in [14] to acquire the broadband second-harmonic spectra. Time domain HOT SPIDER is free of detector array, but remains subject to the requirement of a sufficiently broad phase-matching bandwidth. The system is further complicated by a time-consuming data acquisition process (involving three correlation traces), the insertion of a third path to generate a highly chirped reference pulse, and the employment of a chopper driven in synchronization with the test pulse train (thus difficult to measure high-repetition rate pulses) [15].

The incomplete information shown in the previous literatures suggests that the sensitivities (defined as the peak power times average power of the minimum detectable signal sent into the setup) of the aforementioned nonlinear MIR pulse measurement techniques [4,5,7–10,13,14] are in the order of 10^4 W² (1 μ J, 1 kHz, 100 fs), managing to measure pulses from mode-locked oscillators (3.8 nJ, 145 MHz, 69 fs in [11], 3.3 nJ, 121 MHz, 180 fs in [12]), but are insufficient to characterize the pulses obtained by intra-pulse difference frequency generation (DFG) of an ultra-broadband oscillator (used in seeding an optical parametric chirped pulse amplifier) [16].

In this Letter, we report a high-sensitivity (3×10^{-2} W²) self-referenced noniterative MIR (3.3 μ m) pulse measurement by using a modified interferometric field autocorrelation (MIFA) method. MIFA has been used in measuring ultraweak \sim 400 fs pulses in the telecommunications band [17] and few-cycle pulses (7.2–8.1 fs) centered at 600 [18] and 800 nm [19], respectively. Here we further demonstrate its great flexibility in selecting the SHG crystal and exemption from using a costly NIR (or even MIR) detector array, which are particularly attractive in measuring ultrashort ultraweak MIR pulses. Our experiments successfully retrieved a 3.3 μ m, 43 MHz, \sim 100 fs pulse at

energies down to 8.9 pJ. The feasibility of MIR MIFA was verified by comparing it with the results arising from an SHG FROG and simulation for the spectral phase modulation because of a 4 mm thick Germanium (Ge) plate.

As elucidated in [17–20], the spectral phase function $\psi(f)$ can be reconstructed by acquiring two correlation (MIFA) traces $S_{1,2}(\tau)$ because of spectral sampling at two slightly different second-harmonic frequencies, respectively. The nonlinear spectral sampling can be realized by using (1) a very thick SHG crystal with a δ -like phase-matching spectrum (provided the fundamental pulse itself is only slightly distorted by dispersion) [17,18,20], or (2) a spectrometer after the SHG crystal [19]. The former scheme has a simpler configuration and better sensitivity, but needs to use two crystals [18] or tune the crystal temperature (or orientation) [17,20] to acquire the two MIFA traces. Besides, the trade-off between narrow phase-matching bandwidth (required by MIFA) and small group delay dispersion (required by all nonlinear pulse measurement methods) could result in no adequate crystal thickness (discussed later). We chose the latter scheme in an attempt to measure MIR pulses of very different widths by the same setup.

Figure 1 shows the experimental setup. The 43 MHz, 5 mW (116 pJ), 3.3 μm MIR pulse train came from DFG between two locked ultrafast Yb (1.05 μm) and Er (1.56 μm) fiber lasers in a 2 mm long periodically poled lithium niobate (PPLN) crystal [21]. It was sent into a collinear Michelson interferometer (MI) with a compensating plate (to balance the chirp introduced by the two MI arms) and fringe correction functionality (enabled by a CW laser at 1547 nm and an InGaAs photodetector PD1). The output MIR beam was sent either to a PbSe photodetector PD2 (P4639, Hamamatsu) for MIR power spectrum measurement by using the FTIR technique (thus exempt from an independent MIR spectrometer) or focused into a 266 μm thick AgGaSe₂ crystal ($d_{\text{eff}} = 35.1 \text{ pm/V}$, type I) for SHG. The second-harmonic beam was sent into a homemade spectrometer composed of a grating (1100 gr/mm), a lens L3 ($f = 8 \text{ cm}$), a slit (300 μm), a TE-cooled InGaAs point photodetector PD3 (PB 4206, Teledyne Judson Technologies), and a translation stage TS2. Two MIFA traces were acquired sequentially by reading the PD3 signal via a lock-in amplifier (PCI-4462, National Instruments) with a modulation frequency of 280 Hz at two slightly different slit positions. When performing an SHG FROG (for comparison), the

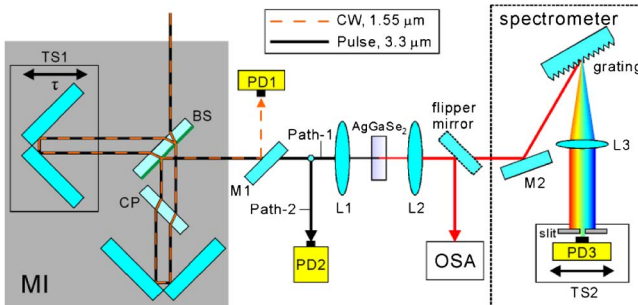


Fig. 1. Experimental setup. MI, Michelson interferometer; TS#, translation stage; BS, beam splitter; CP, compensating plate; PD#, photodetector; M#, mirror; L#, lens.

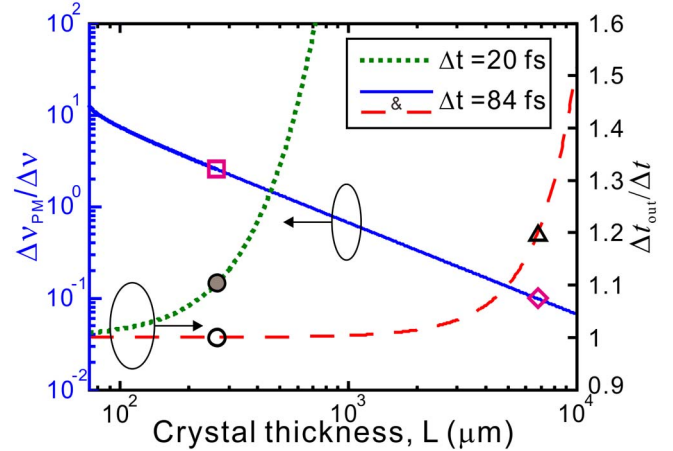


Fig. 2. Normalized phase-matching bandwidth (solid) and normalized output pulse width (dashed) because of different AgGaSe₂ lengths assuming a transform-limited (TL) input pulse of fundamental bandwidth $\Delta\nu$ (3.28 THz) and pulse width Δt (84 fs), respectively. The dotted curve is obtained by assuming a TL Gaussian input pulse of Δt (20 fs) duration.

second-harmonic beam was directed to an optical spectrum analyzer (OSA) by a flipper mirror instead.

Figure 2 shows the impacts of AgGaSe₂ crystal thickness L on the phase-matching bandwidth $\Delta\nu_{\text{PM}}$ (solid) and output fundamental pulse width Δt_{out} broadened by dispersion (dashed) assuming a transform-limited (TL) input pulse with a power spectrum the same as that obtained in our experiment [Fig. 4(g), shaded]. For clarity, $\Delta\nu_{\text{PM}}$ and Δt_{out} are normalized to the fundamental bandwidth $\Delta\nu$ (3.28 THz) and TL pulse width Δt (84 fs), respectively. The four quantities about “width” are defined by full width at half-maximum (FWHM). It is found that $\Delta t_{\text{out}} = 1.0003\Delta t$ (open circle) and $\Delta\nu_{\text{PM}} = 2.54\Delta\nu$ (square) at the chosen crystal thickness ($L = 266 \mu\text{m}$). In other words, our crystal is thin enough to suppress the dispersion-induced pulse broadening, but not thick enough to provide the nonlinear spectral sampling for MIFA measurement. If the crystal thickness is increased to 6.7 mm such that the phase-matching spectrum is sufficiently close to a δ -function [$\Delta\nu_{\text{PM}} = 0.1\Delta\nu$ (diamond)], the fundamental pulse will be noticeably stretched by 19% [$\Delta t_{\text{out}} = 1.19\Delta t$ (triangle)]. As a result, a spectrometer is essential for MIFA measurement under our working conditions, and the crystal thickness is limited only by the dispersion-induced pulse broadening. The dotted curve shows that a TL Gaussian input pulse of 20 fs width will be broadened only by 10% (filled circle) because of the dispersion of a 266 μm thick AgGaSe₂ crystal. It suggests that our current setup is readily applicable to measuring a 3.3 μm pulse down to 20 fs duration.

Figure 3 illustrates the experimentally measured second-harmonic power spectrum (solid) and two spectral slices (shaded) centered at 1605 nm (Slice 1) and 1609 nm (Slice 2), respectively, (all were taken by blocking one of the two MI arms). The homemade spectrometer covers a spectral window of 1548–1695 nm and has a resolution of 1.45 nm (170 GHz) around the two slices. The slice width is only 5% of the fundamental bandwidth $\Delta\nu$ (3.28 THz) or 2.35% of the second-harmonic bandwidth $\Delta\nu_{\text{SH}}$ (7.22 THz), enabling accurate MIFA measurement.

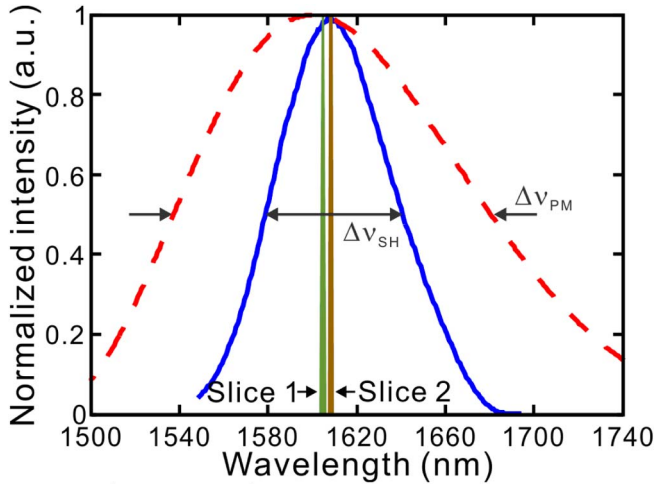


Fig. 3. Experimentally measured second-harmonic power spectrum (solid) and two spectral slices at 1605 nm (Slice 1) and 1609 nm (Slice 2) used in acquiring two MIFA traces. Simulated phase-matching power spectrum (dashed) because of a 266 μm thick AgGaSe₂ crystal.

On the other hand, the measured second-harmonic power spectrum (solid) is filtered by the insufficient phase-matching bandwidth, for the simulated nonlinear polarization bandwidth (assuming a TL pulse with the experimentally measured fundamental power spectrum) is $\sim 2\Delta\nu_{\text{SH}}$. This is one of the reasons that a 200 μm thick AgGaS₂ crystal was used in [14] at the cost of lower d_{eff} value (9.11 pm/V versus 35.1 pm/V of AgGaSe₂), and the frequency-marginal correction process [22] has to be employed in our SHG FROG experiment.

In the first experiment, we retrieved the spectral phase modulation $\psi_{\text{Ge}}(f)$ because of a 4 mm thick Ge plate by MIFA and SHG FROG. Figures 4(a)–4(d) show the MIFA traces acquired before [Figs. 4(a) and 4(b)] and after [Figs. 4(c) and 4(d)] the insertion of the Ge plate. By subtracting the two spectral phases retrieved by MIFA, we got the desired $\psi_{\text{Ge}}(f)$ [Fig. 4(g), dashed]. The same strategy was used in our SHG FROG experiment, where an OSA replaced the homemade spectrometer for data acquisition. The acquired interferometric FROG traces were processed by the standard procedures [23] and corrected by a frequency marginal method [22]. Figure 4(e) illustrates the measured (left panel) and retrieved (right panel) FROG traces before the Ge plate, while Fig. 4(f) is the counterpart of Fig. 4(e) after the Ge plate. The FROG errors in the two measurements are 0.0025 and 0.0031. The difference between the two FROG-retrieved spectral phase functions, i.e., $\psi_{\text{Ge}}(f)$, is displayed in Fig. 4(g) (dotted). The spectral phase modulation functions retrieved by MIFA and FROG are in acceptable agreement with that obtained by simulation [Fig. 4(g), solid] using the Sellmeier equation [24]. The corresponding RMS phase errors [25] are 0.066 rad (MIFA) and 0.175 rad (FROG), respectively.

The chirp of our MIR pulse varies with the chirp rates of and relative delay between the two pulses produced by the two locked fiber lasers. Figure 5 shows the experimentally measured spectral phase ψ_1 (solid) and the corresponding temporal intensity (inset) of the shortest pulse generated by our MIR source. The retrieved

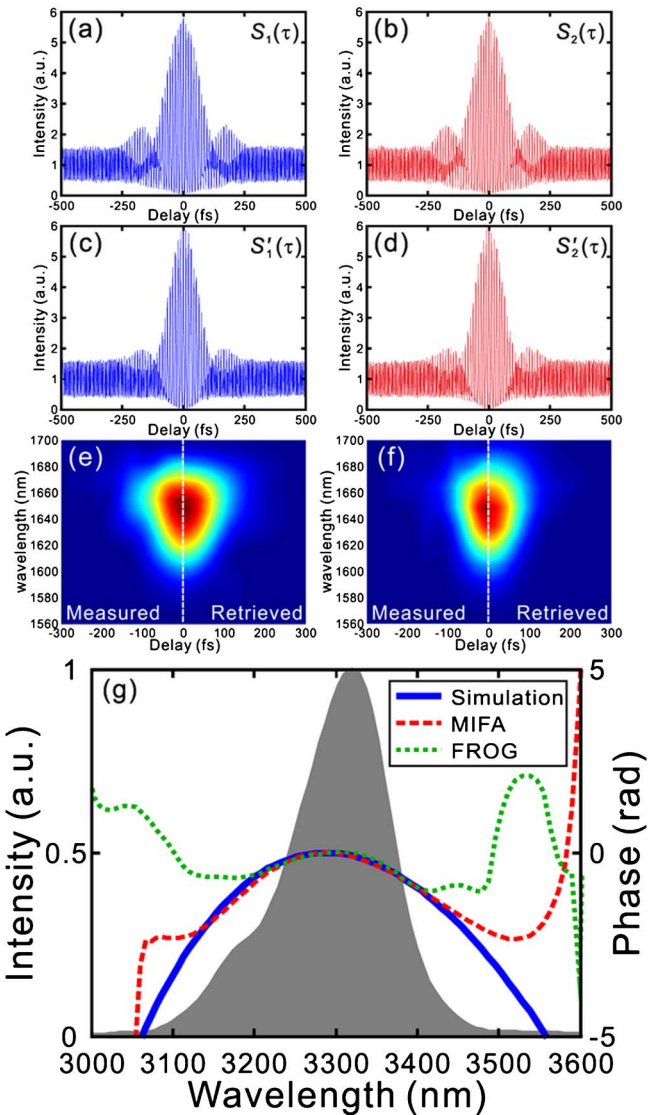


Fig. 4. Measured MIFA traces at (a) 1605 nm and (b) 1609 nm before the 4 mm thick Ge plate. (e) Measured (left panel) and retrieved (right panel) FROG traces before the Ge plate. (c), (d), and (f) are the counterparts of (a), (b), and (e) after the 4 mm thick Ge plate. (g) Experimentally measured power spectrum (shaded) and spectral phases obtained by simulation (solid), MIFA (dashed), and FROG (dotted), respectively.

pulse width is 92 fs (8.4 optical cycles), differing from the TL pulse width (84 fs) by only 10%.

To test the sensitivity of our measurement system, we gradually attenuated the MIR pulse energy for MIFA measurement. Figure 5 also shows the retrieved spectral phases ψ_2 when the pulse energies sent into the MI were 100 pJ (dashed) and 8.9 pJ (dotted), respectively. The two curves are in good agreement, although the input fundamental powers differed by a factor of 11 (second-harmonic powers differed by 126 times). The corresponding average and peak powers of the 8.9 pJ case is 383 μW and 80 W, giving a quadratic measurement sensitivity of $3.1 \times 10^{-2} \text{ W}^2$. The number is reduced to $1.9 \times 10^{-3} \text{ W}^2$ if the pulse energy sent into the nonlinear crystal is taken into account.

In summary, we successfully measured the spectral phase of 43 MHz, ~ 100 fs (8–9 cycles), 3.3 μm MIR pulses

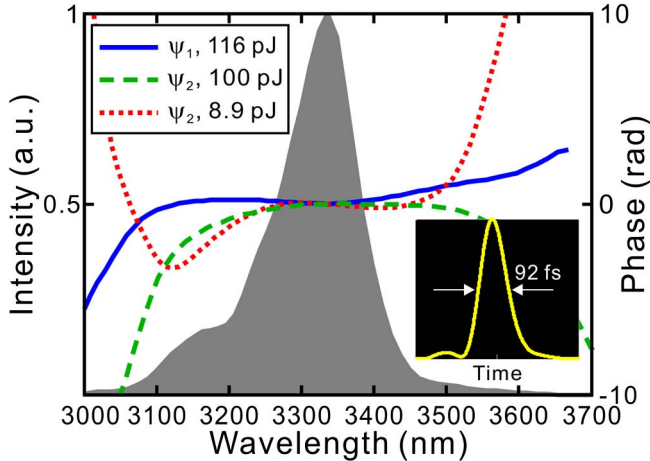


Fig. 5. Experimentally measured power spectrum (shaded) and spectral phase ψ_1 (solid) of a nearly TL pulse of 92 fs width (inset). The spectral phase ψ_2 of another pulse is retrieved at pulse energies of 100 pJ (dashed) and 8.9 pJ (dotted), respectively.

at energies down to 8.9 pJ by the self-referenced noniterative MIFA method. The feasibility is verified by comparing it with the results obtained by FROG and simulation for the spectral phase modulation because of a 4 mm thick Ge plate. To the best of our knowledge, this is the first self-referenced pulse shape measurement for a high-repetition rate (tens of megahertz), low-energy (picojoules) MIR source. The high sensitivity is attributed to the simultaneous employment of a thick SHG crystal of large nonlinear coefficient, sensitive NIR point detector, and lock-in amplifier, which is only made possible by the MIFA method. The access of a narrowband second-harmonic signal permits the use of a photodetector only sensitive to a subset of the second-harmonic spectral range, greatly facilitating the choice of photodetector in MIR pulse measurement (e.g., an InGaAs detector with 1.7 μm cut-off wavelength would not work for SHG FROG if the MIR spectral center is above 3.4 μm , while it could be applicable for MIFA). Our current setup is readily applicable to measuring 3.3 μm pulses down to 20 fs duration (limited by dispersion-induced fundamental pulse broadening because of the 266 μm thick AgGaSe₂ crystal).

We thank HC Photonics for providing the PPLN crystal. This work was supported by the Ministry of Science and Technology of Taiwan under grant MOST 103-2221-E-007-056.

References

1. M.-C. Chen, C. Mancuso, C. Hernández-García, F. Dollar, B. Galloway, D. Popmintchev, P.-C. Huang, B. Walker, L. Plaja, A. A. Jaroní-Becker, A. Becker, M. M. Murnane, H. C. Kapteyn, and T. Popmintchev, Proc. Natl. Acad. Sci. USA **111**, E2361 (2014).
2. Y. H. Wang, H. Steinberg, P. Jarillo-Herrero, and N. Gedik, Science **342**, 453 (2013).
3. S. H. Shim, D. B. Strasfeld, Y. L. Ling, and M. T. Zanni, Proc. Natl. Acad. Sci. USA **104**, 14197 (2007).
4. K. F. Lee, K. J. Kubarych, A. Bonvalet, and M. Joffre, J. Opt. Soc. Am. B **25**, A54 (2008).
5. R. A. Kaindl, M. Wurm, K. Reimann, P. Hamm, A. M. Weiner, and M. Woerner, J. Opt. Soc. Am. B **17**, 2086 (2000).
6. C. Kübler, R. Huber, S. Tübel, and A. Leitenstorfer, Appl. Phys. Lett. **85**, 3360 (2004).
7. D. T. Reid, P. Loza-Alvarez, C. T. A. Brown, T. Beddard, and W. Sibbett, Opt. Lett. **25**, 1478 (2000).
8. M. Tsubouchi and T. Momose, Opt. Lett. **34**, 2447 (2009).
9. T. Fuji and T. Suzuki, Opt. Lett. **32**, 3330 (2007).
10. K. J. Kubarych, M. Joffre, A. Moore, N. Belabas, and D. M. Jonas, Opt. Lett. **30**, 1228 (2005).
11. N. Tolstik, E. Sorokin, and I. T. Sorokina, Opt. Lett. **38**, 299 (2013).
12. A. A. Lagatsky, O. L. Antipov, and W. Sibbett, Opt. Express **20**, 19349 (2012).
13. H. Wang and A. M. Weiner, IEEE J. Quantum Electron. **40**, 937 (2004).
14. P. K. Bates, O. Chalus, and J. Biegert, Opt. Lett. **35**, 1377 (2010).
15. C. Ventalon, J. M. Fraser, J.-P. Likforman, D. M. Villeneuve, P. B. Corkum, and M. Joffre, J. Opt. Soc. Am. B **23**, 332 (2006).
16. K.-H. Hong, S.-W. Huang, J. Moses, X. Fu, C.-J. Lai, G. Cirmi, A. Sell, E. Granados, P. Keathley, and F. X. Kärtner, Opt. Express **19**, 15538 (2011).
17. C.-S. Hsu, H.-C. Chiang, H.-P. Chuang, C.-B. Huang, and S.-D. Yang, Opt. Lett. **36**, 2611 (2011).
18. C.-S. Hsu, Y.-H. Lee, A. Yabushita, T. Kobayashi, and S.-D. Yang, Opt. Lett. **36**, 2041 (2011).
19. C.-Z. Weng, A. H. Kung, and S.-D. Yang, Conference on Lasers and Electro-Optics (Optical Society of America, 2014), paper JTu4A.84te.
20. S.-D. Yang, C.-S. Hsu, S.-L. Lin, H. Miao, C.-B. Huang, and A. M. Weiner, Opt. Express **16**, 20617 (2008).
21. B.-W. Tsai, S.-Y. Wu, C. Hu, W.-W. Hsiang, and Y. Lai, Opt. Lett. **38**, 3456 (2013).
22. G. Taft, A. Rundquist, M. M. Murnane, I. P. Christov, H. C. Kapteyn, K. W. DeLong, D. N. Fittinghoff, M. A. Krumbügel, J. N. Sweetser, and R. Trebino, IEEE J. Sel. Top. Quantum Electron. **2**, 575 (1996).
23. G. Stibenz and G. Steinmeyer, Opt. Express **13**, 2617 (2005).
24. M. Bass, C. DeCusatis, J. M. Enoch, V. Lakshminarayanan, G. Li, C. MacDonald, V. N. Mahajan, and E. V. Stryland, *Handbook of Optics, Volume IV: Optical Properties of Materials, Nonlinear Optics, Quantum Optics*, 3rd ed. (McGraw-Hill, 2009).
25. D. N. Fittinghoff, K. W. DeLong, R. Trebino, and C. L. Ladera, J. Opt. Soc. Am. B **12**, 1955 (1995).